O-shell emission of heavy atoms in an optically thin tokamak plasma

M. Finkenthal,* S. Lippmann,† L. K. Huang, A. Zwicker, and H. W. Moos
Department of Physics and Astronomy, The Johns Hopkins University, Baltimore, Maryland 21218

W. H. Goldstein and A. L. Osterheld
L-Division, Lawrence Livermore National Laboratory, P.O. Box 808, Livermore, California 94550
(Received 7 November 1991)

Heavy atoms Au ($Z=79$), Pb ($Z=82$), Bi ($Z=83$), and U ($Z=92$) have been introduced in the low-density ($n_e \sim 10^{13}$ cm^{-3}) high-temperature ($T_e \geq 1$ keV) TEXT tokamak (Fusion Research Center, University of Texas at Austin) plasma. The emission has been measured in the 50–200-Å range using a photometrically calibrated, time-resolving grazing-incidence spectrometer. The *O*-shell ion emission has been identified by comparison with *ab initio* energy-level calculations and line-intensity predictions of collisional radiative models for various charge states with $5p^6 5d^k$ ground-state configurations.

PACS number(s): 52.25.Nr, 32.30.Rj, 52.70.La

I. INTRODUCTION

The soft-x-ray emission of highly charged heavy ions has been extensively studied in connection with laser-driven inertial confinement experiments and x-ray laser research, and in search of sources for x-ray microscopy and lithography. Most soft-x-ray spectra were obtained from laser-produced plasmas in which the scaling of the x-ray conversion efficiency was studied as a function of the laser-pulse width, wavelength, and the power density on the target [1]. Although in some of these experiments it was not essential to identify specific charge states and transitions, in many laser-produced plasma experiments unambiguous identification is important. In fact, even in experiments aimed primarily at producing efficient x-ray sources, it is useful to determine the charge-state distributions in order to optimize these sources.

The main difficulties related to these objectives stem from the effects of the high density on the emission patterns: doubly excited states tend to be heavily populated and complicate the line spectra of the emitting ions, and the optical thickness of many transitions smears the spectra into broad quasicontinuous features. If one adds to these effects the fact that most laser-produced x-ray spectra obtained are time integrated, one sees the difficulty in identifying the emitting charge states and the various transitions from which lines originate.

The present work overcame these problems by producing the soft-x-ray spectra of heavy atoms Au, Pb, Bi, and U in a high-temperature but low-density tokamak plasma. Moreover, since both the plasma lifetime and the characteristic times for spectral emission were very long (tens or hundreds of milliseconds), it was possible to follow the time-resolved emission from this optically thin plasma under coronal conditions.

The comparison of the experimental spectra with *ab initio* level energy computations and line intensities predicted by collisional radiative models leads to the conclusion that, for all elements under discussion, as many as 18 charge states emit lines originating mainly from $5s^2 5p^k$-$5s 5p^{k+1}$, $5p^k$-$5p^{k-1}5d$, $5p^6 5d^k$-$5p^5 5d^{k+1}$, and $5d^k$-$5d^{k-1}5f$ transitions in relatively narrow spectral bands. The isoelectronic trends of these transitions have been studied and the results are discussed in connection with various applications mentioned above.

II. EXPERIMENT

The atoms of interest were introduced in the TEXT tokamak (Fusion Research Center, University of Texas at Austin) plasma during the steady-state phase of the discharge. The central electron density varied between 2 and 4×10^{13} cm^{-3} and the electron temperature varied between 800 and 1200 eV in hydrogen discharges. Other experimental parameters and the effect of the injection on the target plasma were reported in a previous paper on the uranium emission from TEXT [2].

The spectra were recorded by means of a 2-m grazing-incidence time-resolving spectrometer, GRITS [3], provided with an image intensifier detector. The instrument had been previously calibrated photometrically on the synchrotron ultraviolet radiation facility (SURF II) at NIST; the wavelength calibration has been obtained by using intrinsic oxygen, carbon, titanium, and iron lines emitted from the tokamak plasma in the spectral range 50–200 Å. In every discharge a spectral range of between 50 and 80 Å was recorded simultaneously, with a time resolution of 13 msec. The spectral resolution in the experiments under discussion was 0.7 Å. The accuracy of the measured wavelengths was ±0.2 Å.

The present work describes injections of Au, Pb, Bi, and U atoms into hydrogen plasmas only, although, in order to see the effect on the emission of increasing the temperature, we have injected Au into deuterium and U into hydrogen, deuterium, and helium plasmas. The elements of interest, introduced into the tokamak by a laser blow-off technique, emitted for 70–90 msec following injection. The steady-state phase of the tokamak discharge was about 300 msec. Figure 1 shows three successive frames during lead injections. The background radiation

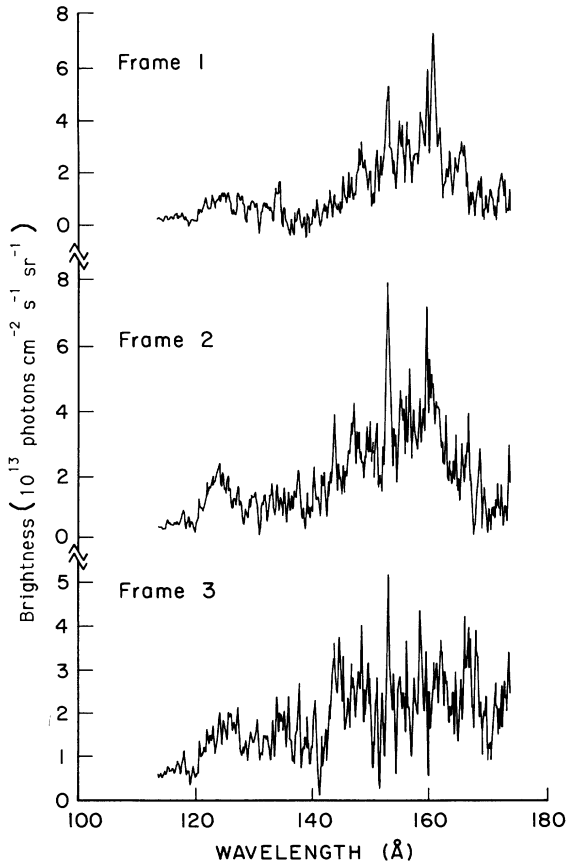

FIG. 1. Three successive frames during lead injections in TEXT. The background radiation has been subtracted to obtain pure Pb spectra. The quasicontinuous emission bands originate from ions with $5p^k$ and $5d^k$ ground-state configurations.

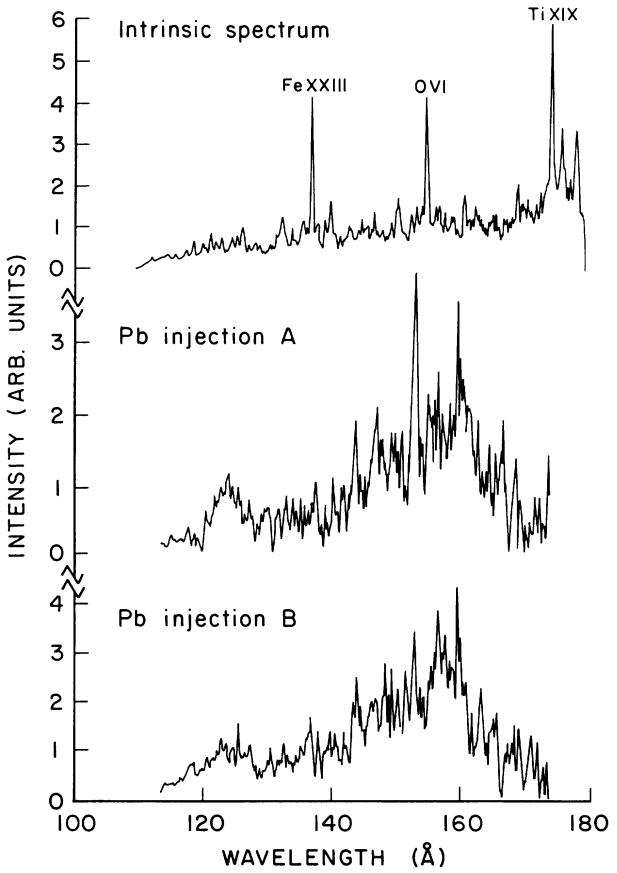

FIG. 2. The top trace is the intrinsic spectrum, prior to Pb injection, dominated by oxygen, iron, and titanium line emission. The two lower spectra are frames taken at the same time after the lead injection, in two different tokamak discharges.

has been subtracted, so that the spectra are due only to lead. A few strong $5s$-$5p$ lines emitted by ions having simple ground-state configurations (Pm I– and Sm I–like having $4f^{13}5s$ and $4f^{13}5s^2$ ground-state configurations) stand out on top of a narrow, quasicontinuous emission band originating from ions with $5p^k$ and $5d^k$ ground configurations (see discussion in Sec. IV). Figure 2 shows the reproducibility of these results: the top trace is the intrinsic spectrum in the same range, previous to the Pb injection; it is dominated by oxygen, iron, and titanium line emission, and the background "noise" is low. The two lower spectra are frames taken at the same time after the lead injection in two different tokamak discharges. Gold, bismuth, and uranium spectra show the same general characteristics. Figure 3 shows a fragment of the gold spectrum together with the background emission in the 115–170-Å region. The uranium emission of the corresponding charge state, shown in Fig. 4, has been presented in our previous work [2].

III. *AB INITIO* ATOMIC STRUCTURE CALCULATIONS AND COLLISIONAL RADIATIVE MODELS

Ab initio atomic structure and collisional radiative calculations were carried out using the HULLAC package of

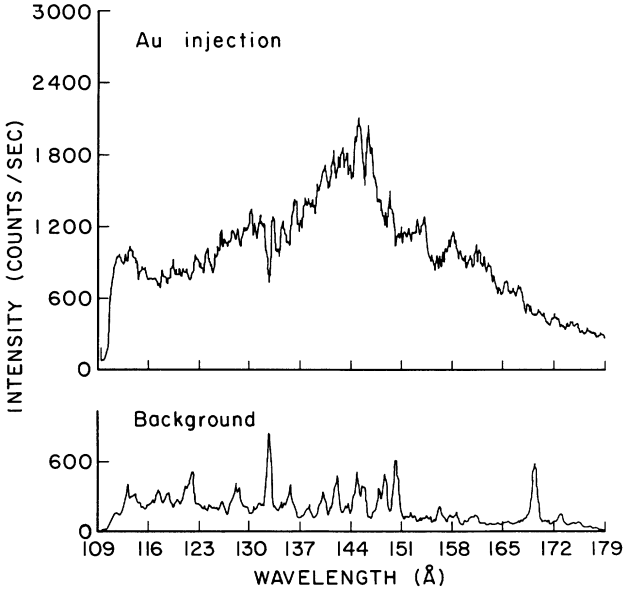

FIG. 3. A fragment of the gold spectrum together with the background emission in the 115–170-Å region.

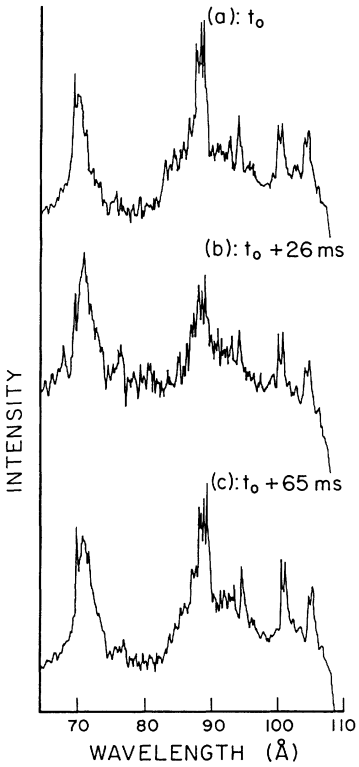

FIG. 4. Coronal *O*-shell emission in uranium, from Ref. [2]. Owing to a configuration interaction, the $5p_{1/2,3/2}$-$5d$ and $5d$-$5f$ transitions produce only two bands, centered at 70 and 90 Å.

computer programs developed over the past several years at Hebrew University and the Lawrence Livermore Laboratory. This package is based on the relativistic parametric potential model [4] and the distorted-wave approximation for collisional processes [5]. It was specifically designed to compute the atomic physics of highly charged heavy elements. Results from this package have been reported extensively [6].

The programs that constitute HULLAC include ANGLAR, based on the graphical angular recoupling program NJGRAF [7], which generates fine-structure levels in a j-j coupling scheme for a set of user-specified electron configurations, and computes the angular part of the Hamiltonian and of the tensor operators for radiative and collisional transitions; RELAC, the relativistic version of MAPPAC [4], which computes wave functions, energies, and spontaneous-transition probabilities; and CROSS, a suite of three codes that compute distorted-wave collisional transition cross sections and rate coefficients, including exchange and configuration interaction, using target relativistic wave functions generated by RELAC [5]. Data from these codes generate a collisional radiative model that is solved for level populations and line emissivities by assuming steady-state conditions.

The collisional radiative calculations presented here included the 283 levels belonging to the $5p^6 5l$ and $5p^5 5d\,5l$, $l=d,f,g$, Tm I–like configurations; the 1149 levels of the $5p^6 5d\,5l$ and $5p^5 5d^2 5l$, Yb I–like configurations; the 1445 levels of the $5p^6 5d^7 5l$ and $5p^5 5d^8 5l$, Os I–like configurations; and the 405 levels of the $5p^6 5d^8 5l$ and $5p^5 5d^9 5l$, Ir I–like configurations. All radiative electric dipole decays and collisions between these levels have been included in the models. Thus, the models are applicable in both low-density tokamak and high-density laser-produced plasma regimes.

Calculations are presented here for an electron density of 10^{13} cm^{-3}, and have been found to be substantially insensitive to variations of up to a factor of 10 about this value. Calculated spectra are also relatively insensitive to electron-temperature variations, for temperatures above the excitation energy for the 5-5 transitions in these ions, $\sim$50–200 eV. Threshold effects appear at lower temperatures as a variation in the relative intensities of the various emission bands associated with $5p_{1/2,3/2}$-$5d$ and $5d$-$5f$ transitions. This sensitivity may help explain the ratios observed in this experiment, though additional effects must be taken into account (see Sec. IV). We have calculated level populations and line intensities at temperatures corresponding roughly to $\frac{1}{3}$ the ionization potential for ions with half-filled $5d$ shells, viz., 50 eV for lead and 200 eV for uranium.

IV. RESULTS AND DISCUSSION

Soft-x-ray spectra of heavy atoms ($Z>70$) emitted from tokamaks having tungsten or gold limiters have been observed in experiments using the Princeton large torus (PLT [8], the tokamak at the Oak Ridge National Laboratory (ORMAK) [9], and the DIVA [10] facility. In previous experiments on TEXT, we injected W, Au, Ti, and Pb to observe $n=4$ to 4 transitions originating from N-shell ions between 20 and 60 Å [11,12].

Due to the lack of strong individual lines of various charge states, it is difficult to establish for these high-Z atoms whether the charge-state distribution corresponds to an ionization equilibrium (IE) situation or not. (Fast radial transport of the ions may produce deviations from IE although the W, Au, and Pb $n=4$ to 4 emission from TEXT indicated that the distribution of the emitting charge states is not significantly different from the equilibrium distribution [11].) The bunching together of the $\Delta n=0$ emission from many charge states, discussed for rare earths W, Au, and U in our previous works [2,11–13], leads to bandlike structure that change very little while the local electron temperature changes. A striking example was the unchanged $n=4$ to 4 Au emission in PLT, at 50–60 Å, with and without hollow temperature profiles (central electron temperatures of 500 and 1500 eV, respectively) [8]. Our previous analysis of uranium spectra from TEXT showed that, in a plasma with $T_e(0)\leq 1000$ eV, charge states as high as U^{31+}, with ionization potentials ≤ 1200 eV, were obtained [2].

The radial electron-temperature profile in TEXT is well approximated by a Gaussian function; the injected atoms penetrate the plasma at the edge and slowly diffuse toward the hot center. The time history of the central uranium emission around 90 Å showed a slow increase during 3–4 frames ($\sim$40–50 msec) and a decrease over 3–4 frames. The rise time is indicative of the inward

diffusion and ionization times and the decay of the signal represents mainly the ion-confinement time (the radiative-recombination times are longer at these high temperatures). Therefore, as ions penetrate the plasma they will pass through all the ionization stages from neutral to the highest. Since we did measure, under the described experimental conditions, N-shell radiation of Au, Pb, and Bi, we can safely assume that all the charge states emitting O-shell radiation will be represented in the detected spectra. In the case of uranium we may assume the same, since individual lines of U^{31+} and U^{32+} lines have been identified in the spectra.

If we use the ionization potentials of the various charge states as upper limits, from comparison of these and the electron-temperature profiles we see that the O-shell ions of Au to Bi emit from the outer half of the plasma. For instance, the ionization potential of Sm I–like Pb^{20+} is 570 eV, whereas that of U^{30+} is 1050 eV. Since, across the steep temperature gradients at the edge, low-ionization states burn through rapidly and the confinement is poorer than in the center, one expects that in the Au spectra, for instance, the predominantly emitting charge states will be those with a few d electrons left in the $5d^k$ subshell and the $5p^k$ ($k=1$ to 6) ions. For Pb and Bi, more contributions from $5d^k$ subshell charge states are expected. In the case of uranium, we expect all the ions having $5p^6 5d^k$ ($k=1$ to 10) ground configurations to contribute to the spectra.

Assuming the above ion distributions, the next step in the analysis is to establish the radiative patterns of these charge states. A common feature of the 16 charge states from Pt I–like (ground $5d^{10}$) to Eu I–like (ground $5p$) is

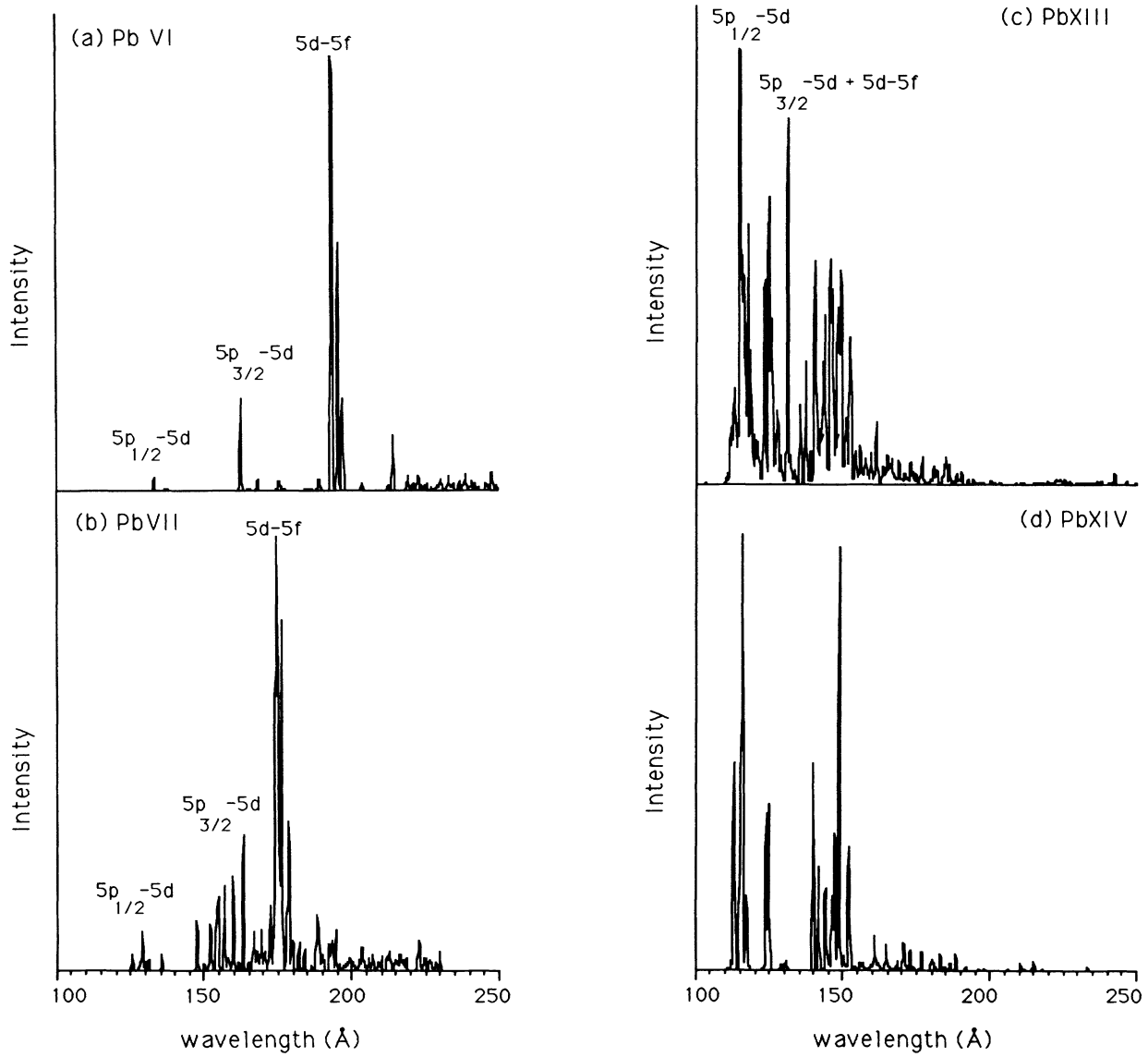

FIG. 5. Synthetic spectra for (a) Pb^{5+}, (b) Pb^{6+}, (c) Pb^{12+}, and (d) Pb^{13+} ions, at an electron temperature of 50 eV, and a density of 10^{13} cm^{-3}. The spectra are based on separate collisional radiative models for each charge state. Ionization and recombination processes are not included. The Gaussian line widths have been arbitrarily set at 0.5 Å.

that their $5p$-$5d$ and $5d$-$5f$ emission will be bunched together in narrow bands of emission. For uranium ions we have shown already [2] that a configuration-interaction effect blends the $5p^6 5d^k$-$(5p^5)_{3/2} 5d^{k+1}$ and $5d^k$-$5d^{k-1}5f$ transitions; thus instead of having three different spectral features corresponding to $5p_{1/2,3/2}$-$5d$ and $5d$-$5f$ transitions, the spectra showed two bands centered at 70 and 90 Å (see Fig. 4).

Figures 5(a)–5(d) show synthetic spectra for, respectively, the Pb^{5+}, Pb^{6+}, Pb^{12+}, and Pb^{13+} ions, at an electron temperature of 50 eV and a density of 10^{13} cm^{-3}; as described in Sec. III, the spectra are based on separate collisional radiative models for each charge state. Ionization and recombination processes are not included. The temperature dependence of these predicted spectra is demonstrated in Fig. 6, where calculations at 200 eV are presented. We will use these ions, with ground configurations $5p^6 5d^k$, $k = 1,2,8,9$, to investigate the emission bands arising from $5p^6 5d^k$-$5p^6 5d^{k-1}5f$ and $5p^6 5d^k$-$5p^5 5d^{k+1}$, $k = 1$–9. The first thing to note is that the combination of these charge states will clearly give rise to all three emission bands, in contradistinction to the U case, but that these bands get very different contributions as the $5d$ shell is filled. Near the empty shell, the $5p_{1/2}$-$5d$ transitions dominate, while the $5d$-$5f$ transitions have virtually vanished. At slightly longer wavelengths, the $5p_{3/2}$-$5d$ lines contribute a second weaker band. As the $5d$ shell fills, the $5d$-$5f$ band migrates to longer wavelengths and finally dominates the spectrum. Meanwhile, the relative strength of the $5p_{1/2}$-$5d$ and $5p_{3/2}$-$5d$ bands reverses. The combined effect of these trends is to generate three bands whose relative magnitudes ought to be sensitive to the charge-state distribution.

The trends observed in Fig. 5 can be attributed, as in the case of U, to the strong configuration interaction that

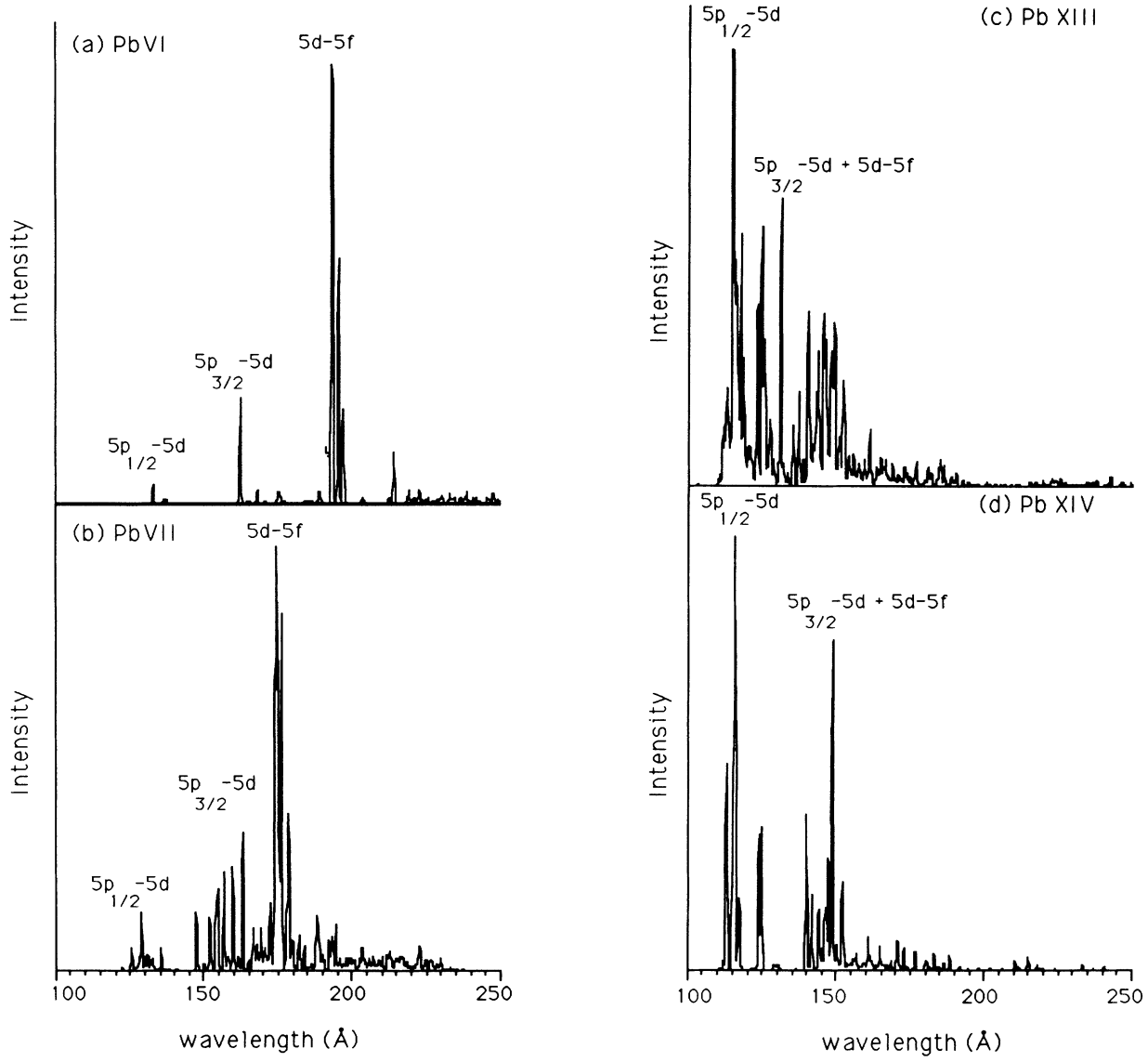

FIG. 6. Same as Fig. 5, but at an electron temperature of 200 eV.

develops between the $5p^6 5d^{k-1} 5f$ and $(5p^5)_{3/2} 5d^{k+1}$ configurations. This mixing is minimal for charge states of lead with nearly full $5d$ shells, where the coupling is almost pure j-j and the energy splitting between the $5p^6 5d^{k-1} 5f$ and $(5p^5)_{3/2} 5d^{k+1}$ is large (~ 1 a.u.). For Pb^{5+}, the $(5p^5)_{3/2} 5d^{10}$ level is 77.3% pure, with a 22.7% admixture of $5p^6 5d^8 5f$. The $5d$-$5f$ transition dominates the $5p$-$5d$ one, owing to the large number of $5d$ electrons relative to holes. By the same token, the oscillator strengths for the $5p^6 5d^9$-$(5p^5)_{3/2} 5d^{10}$, and $5p^6 5d^9$-$(5p^5)_{1/2} 5d^{10}$ transitions stand roughly in the 2:1 ratio of their final-state multiplicities.

As $5d$ electrons are removed, the $5p^6 5d^k 5f$ configurations move to higher energy, becoming nearly degenerate with the $(5p^5)_{3/2} 5d^{k+1}$ ones. (For Tm I–like Pb^{13+} the average configuration splitting is less than 0.003 a.u.) While the $(5p^5)_{1/2} 5d^{k+1}$ configuration remains nearly pure (>85% purity for the strongest $5p^6 5d$-$(5p^5)_{1/2} 5d^2$ transition in Pb^{13+}), the $5p^6 5d^{k-1} 5f$ and $(5p^5)_{3/2} 5d^{k+1}$ configurations become mixed so completely that there is no way to decide to which configuration a level belongs. At this point the $5d$-$5f$ and $5p_{3/2}$-$5d$ bands merge at about 150 Å.

Comparing the model spectra in Fig. 5 with the Pb data shown in Figs. 1 and 2, which shows only two emission bands, we conclude that the charge-state balance in the experiment was weighted towards the empty $5d$ shell. In the recorded spectra above 170 Å there are no prominent lead emission features. This is not surprising since the very-low-charge states Pb^{5+} and Pb^{6+} would be emitted at the edge of the TEXT plasma where, as already indicted, the particle-confinement time is very short and the transport parallel to the toroidal field very fast. As a result, the fractional abundance of these low charge states

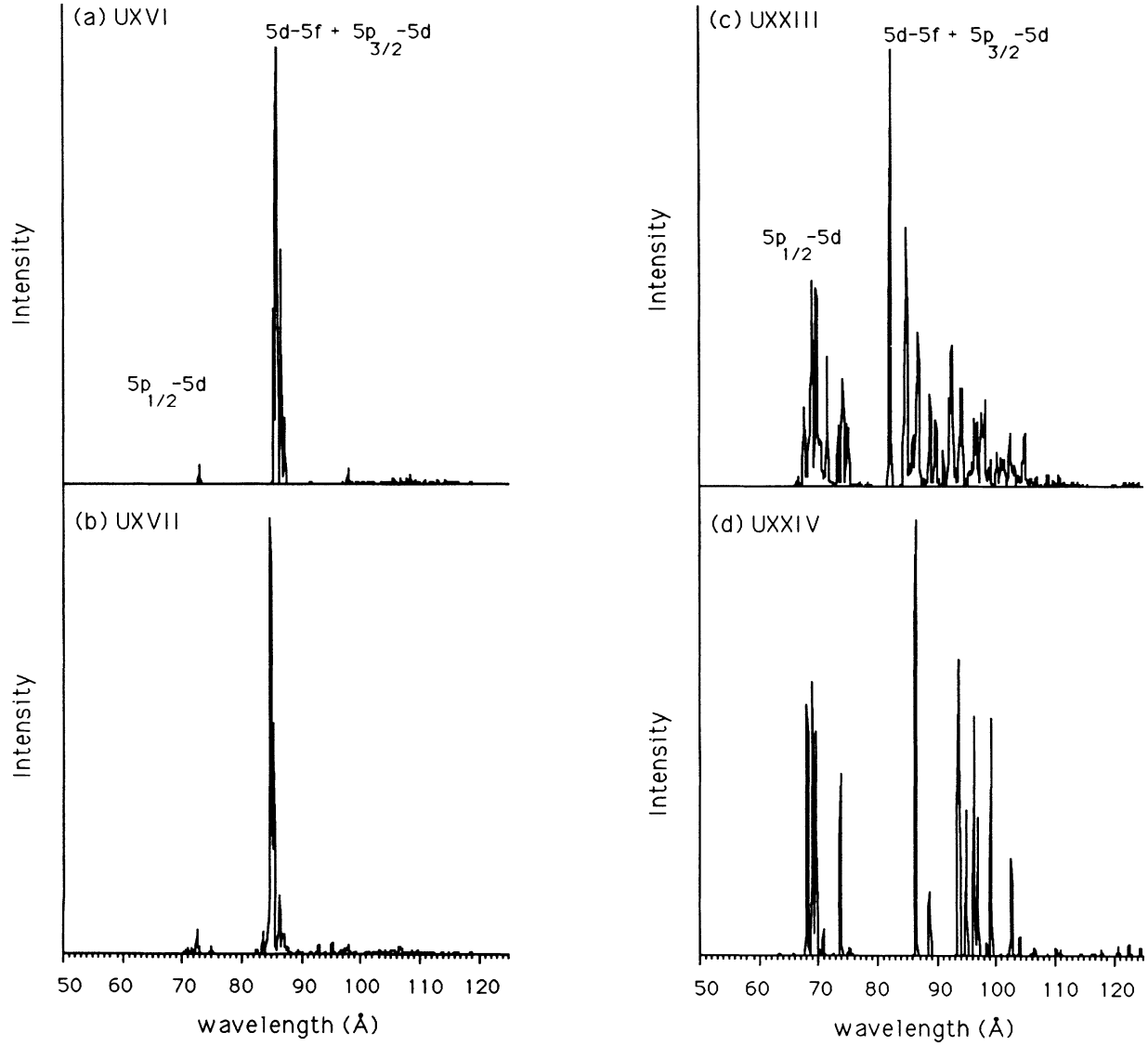

FIG. 7. Collisional radiative calculations for uranium at 200 eV and 10^{13} cm^{-3}. (a) U^{15+}, (b) U^{16+}, (c) U^{22+}, and (d) U^{23+}. The line widths have been arbitrarily set at 0.25 Å.

is much smaller than that of Pb^{12+} and Pb^{13+}.

The relative widths and heights of the observed features centered at roughly 125 and 155 Å in lead cannot be adequately addressed by the present models. These parameters are probably determined by the behavior of intermediate-charge states ($5p^6 5d^k$, $2 < k < 8$), by ions with $5p^k$ ground-state configurations, and by both intrinsic and instrumental blending of the many individual lines that contribute. A treatment of these details awaits either the development of collisional radiative models for charge states through the $5p$ and $5d$ shells, or an unresolved transition-array treatment that includes the effects of configuration interaction.

Finally, Fig. 7 shows collisional radiative calculations for uranium at 200 eV and 10^{13} cm^{-3}. These spectra display trends similar to the Pb: a dominant $5d$-$5f$ transition near the closed shell, gradually losing relative intensity as $5d$ electrons are stripped. But for the more highly stripped uranium, the $5p^6 5d^{k-1} 5f$ and $(5p^5)_{3/2} 5d^{k+1}$ manifolds are nearly degenerate for all k, in contradistinction to the lead case. Thus, only two bands are evident, as pointed out in Ref. [2].

It is worth noting in connection with interpreting the emission patterns of complex ions, especially with a view toward understanding their relation to plasma conditions, that comparisons between data and simple distributions of oscillator strength are not generally sufficient. Instead, it is necessary to apply collisional radiative models, as we have done here, both to extract the maximum information from the spectra and to ensure correct identification of features. As an illustration, we compare in Figs. 7 and 8 two models for the spectra of U^{15+}, U^{16+}, U^{22+}, and U^{23+}. In Fig. 8 are plotted simple oscillator strengths, rather than collisional radiative line intensities. Clearly, except at a very gross level, these latter plots in no way suggest the collisional radiative models, neither in accu-

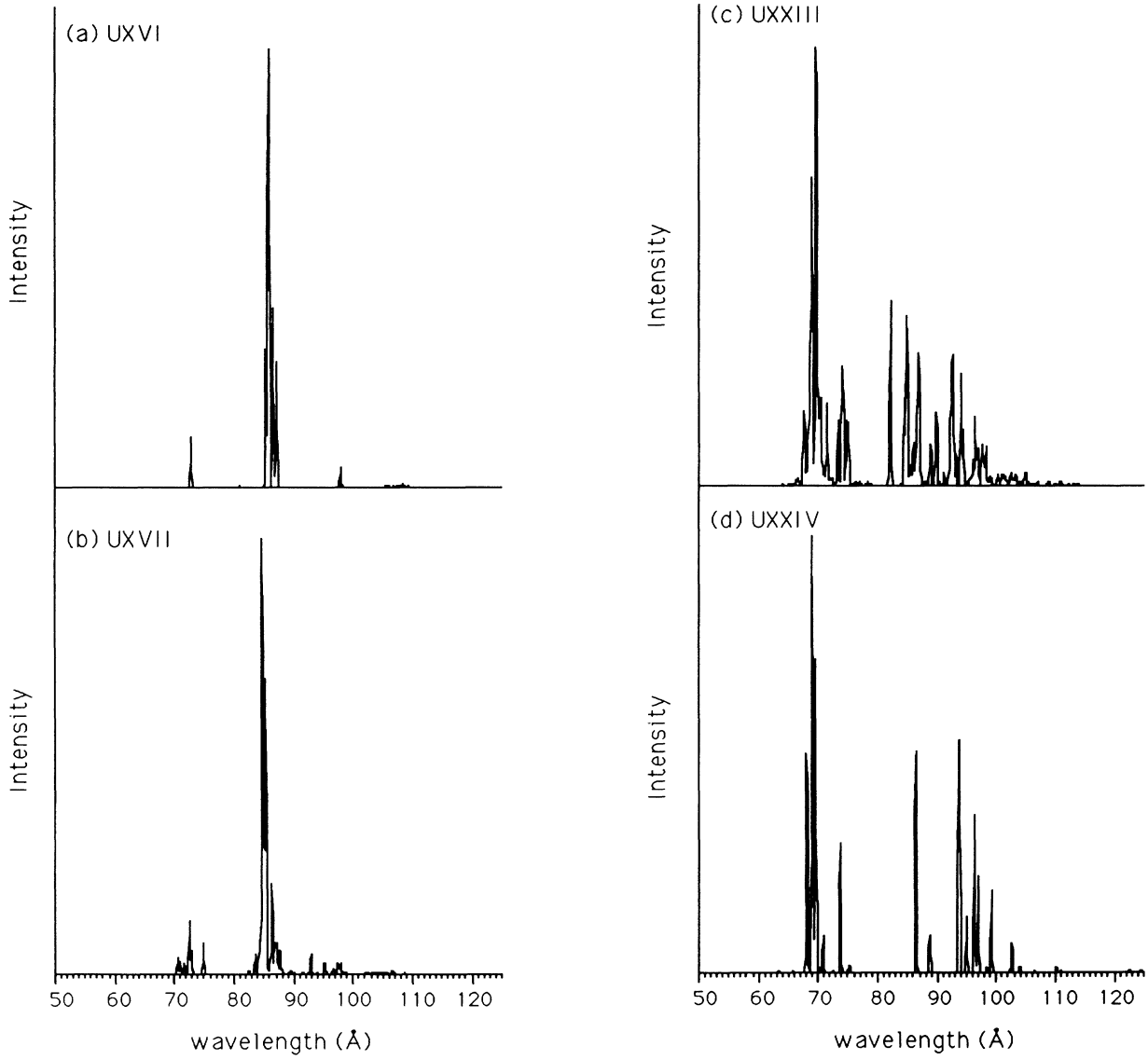

FIG. 8. Oscillator strength for (a) U^{15+}, (b) U^{16+}, (c) U^{22+}, and (d) U^{23+}.

rately locating the position of spectral bands, nor in predicting their relative intensity.

In conclusion, the $n=5$ to 5 transitions emitted from O-shell charge states of gold, lead, bismuth, and uranium from a low-density, high-temperature tokamak plasma have been identified in the 50–200-Å region. *Ab initio* atomic structure computations and line intensities predicted by collisional radiative models have been used to interpret the results. Two relatively narrow bands are emitted by each of these elements in the low-density tokamak spectra; the bands are constituted of lines originating mainly from $5p^6$-$5p^5 5d$, $5p^6 5d^k$-$5p^5 5d^{k+1}$, and $5d^k$-$5d^{k-1}5f$ transitions.

ACKNOWLEDGMENTS

The authors acknowledge the TEXT group, and W. Rowan in particular, for help during the experiments. V. Kaufman of NIST is acknowledged for useful discussions related to the atomic structure of the O-shell charge states.

*Permanent address: Racah Institute of Physics, The Hebrew University, Jerusalem 91904, Israel.

†Present address: General Atomics, San Diego, CA 92138-5608.

[1] See, for example, Proc. SPIE **230** (1988) (special issue on x-rays from laser-produced plasmas).

[2] M. Finkenthal, S. Lippmann, H. W. Moos, P. Mandelbaum, and the TEXT Group, Phys. Rev. A **39**, 3717 (1989).

[3] W. L. Hodge, B. C. Stratton, and H. W. Moos, Rev. Sci. Instrum. **55**, 6 (1984).

[4] M. Klapisch, Comput. Phys. Commun. **2**, 269 (1971); M. Klapisch, J. L. Schwob, B. S. Fraenkel, and J. Oreg, J. Opt. Soc. Am. **67**, 148 (1977).

[5] A. Bar-Shalom, M. Klapisch, and J. Oreg, Phys. Rev. A **38**, 1773 (1988).

[6] M. Klapisch, M. Cohen, W. H. Goldstein, and U. Feldman, Phys. Scr. **41**, 148 (1990), and references therein; P. Beiersdorfer, A. L. Osterheld, M. H. Chen, J. R. Henderson, D. A. Knapp, M. A. Levine, R. E. Marrs, K. J. Reed, M. B. Schneider, and D. A. Vogel, Phys. Rev. Lett. **65**, 1995 (1990).

[7] A. Bar-Shalom and M. Klapisch, Comput. Phys. Commun. **50**, 375 (1988).

[8] E. Hinnov and M. Mattioli, Phys. Lett. **66**, 109 (1978).

[9] R. C. Isler, R. V. Neidigh, and R. I. Cowan, Phys. Lett. **63**, 295 (1977).

[10] S. Kasai, A. Funahashi, M. Nagami, and T. Sugie, Nucl. Fusion **19**, 195 (1979).

[11] M. Finkenthal, L. K. Huang, S. Lippmann, H. W. Moos, P. Mandelbaum, J. L. Schwob, M. Klapisch, and the TEXT Group, Phys. Lett. A **127**, 255 (1988).

[12] M. Finkenthal, S. Lippman, H. W. Moos, and P. Mandelbaum, SPIE **1140**, 162 (1989).

[13] P. Mandelbaum, J. L. Schwob, M. Finkenthal, and M. Klapisch, J. Phys. (Paris) Colloq. **49**, C1-127 (1988).